Technology and Health Care 23 (2015) S239–S247
DOI 10.3233/THC-150959
IOS Press

A complexity-efficient and one-pass image compression algorithm for wireless capsule endoscopy

Gang Liu*, Guozheng Yan, Shaopeng Zhao and Shuai Kuang
Institute of Precise Engineering and Intelligent Microsystems, Shanghai Jiao Tong University, Shanghai, China

Abstract.
BACKGROUND: As an important part of the application-specific integrated circuit (ASIC) in wireless capsule endoscopy (WCE), the efficient compressor is crucial for image transmission and power consumption.
OBJECTIVE: In this paper, a complexity-efficient and one-pass image compression method is proposed for WCE with Bayer format images. The algorithm is modified from the standard lossless algorithm (JPEG-LS).
METHODS: Firstly, a causal interpolation is used to acquire the context template of a current pixel to be encoded, thus determining different encoding modes. Secondly, a gradient predictor, instead of the median predictor, is designed to improve the accuracy of the predictions. Thirdly, the gradient context is quantized to obtain the context index (Q). Eventually, the encoding process is achieved in different modes.
RESULTS: The experimental and comparative results show that our proposed near-lossless compression method provides a high compression rate (2.315) and a high image quality (46.31 dB) compared with other methods.
CONCLUSION: It performs well in the designed wireless capsule system and could be applied in other image fields.

Keywords: Wireless capsule endoscopy (WCE), image compression, one-pass, causal interpolation, gradient predictor

1. Introduction

Wireless capsule endoscopy (WCE) is a state-of-the-art technology that evaluates the entire gastrointestinal (GI) tract with a noninvasive and painless procedure [1]. Given Imaging Company released the first commercialized WCE, which could be easily swallowed by patients [2]. Some other types of CEs, introduced by Olympus, Pentax, and Siemens, are also on the market [3,4]. These capsules consist of a tiny image sensor with LED-based illumination, a processing and controlling unit, a RF transmitter, and small batteries. Due to peristalsis, the capsule moves through the GI tract, capturing images that are then wirelessly transmitted to a storage device worn by the patient. However, they only last for about eight hours and acquire 2 frames per second. To reduce the power consumption and resolve the bottleneck of wireless communication bandwidth, the image compressor of application-specific integrated circuit (ASIC) is crucial in WCE [5–7].

*Corresponding author: Gang Liu, Institute of Precise Engineering and Intelligent Microsystems, Shanghai Jiao Tong University, No. 800 Dongchuan, Minhang district, Shanghai 200240, China. Tel.: +86 21 34204434; Fax: +86 21 34204434; E-mail: liugang531557127@163.com.

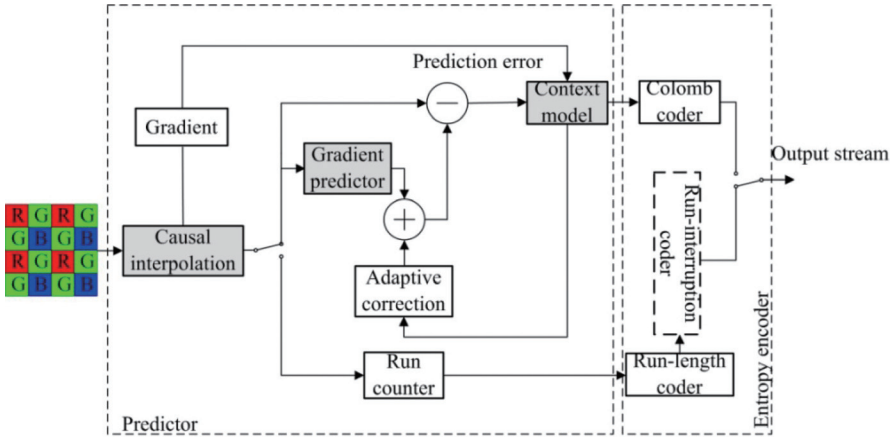

Fig. 1. Flowchart of the proposed method.

At present, there are various studies committed to the future generations of WCE, which capture images in Bayer format, thus reducing the amount of data to one-third [8]. However, with the rapid development of image sensor technology, images with a high frame rate, good quality, and strong resolution in the Bayer pattern still exceed the bandwidth of the transmitter. Many compression methods for images in Bayer format have been presented for higher-compression performance [9–11]. But, these methods allow for some information contained in original images to be lost, resulting in error. There are also a few lossless and high-quality compression methods presented based on structure transformation [5,12–17], but their computation complexity is too high to be adopted in wireless endoscopy application. Moreover, they all belong to multiple-pass compression mechanisms, which are more costly in terms of hardware resources.

Among various existing lossless compression schemes, JPEG-LS is the ITU/ISO standard for lossless image compression. It is ideal for hardware implementation because of its relatively low complexity algorithm, low storage requirement, efficient compression capabilities. The WCE images have similar backgrounds, while the medical diagnosis on these images could be represented by some the specific color and texture. So, JPEG-LS is suitable for WCE images. However, the efficiency of JPEG-LS directly used to compress Bayer images is too low, due to poor spatial correlation of adjacent pixels. So, a series of improvements must be proposed. In the present study, a complexity-efficient and one-pass image compression method, modified from JPEG-LS, is proposed for WCE with Bayer format images. In order to achieve this mechanism, a causal interpolation should be used to acquire pixels of the same color as the pixel to be encoded. Then, a gradient predictor is designed in regular mode to improve the prediction accuracy. The gradient context is re-quantized to obtain the optimum quantization interval. Figure 1 shows the flowchart of the proposed method. With these designs, the proposed near-lossless compression method provides a high compression rate and high image quality.

2. Materials and methods

2.1. Causal interpolation of the current pixel

In order to fully reflect the statistical features of the current coding pixels, an extended context template is adopted, shown in Fig. 2(a). The pixels in the context template must be the same color as the current

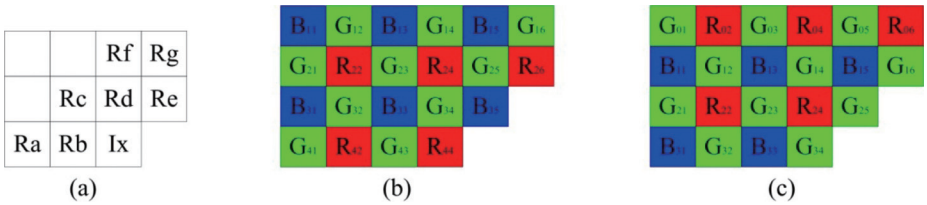

Fig. 2. The causal template of the current pixel: (a) context template, (b) causal interpolation of R (B), (c) causal interpolation of G.

pixels. Causal interpolation is thus proposed in the location Ra-Rf. In view of the different primary colors of the current pixel, different manners are adopted:

(1) For R primary color pixels, the interpolation template is shown in Fig. 2(b). The estimate of R color pixels in the context template are given by:

$$\begin{aligned} R_a &= R_{42} & R_b &= \widetilde{R}_{43} = R_{42} + \frac{G_{43} - G_{41}}{2} \\ R_c &= \widetilde{R}_{33} = \frac{2R_{22} + R_{24} + R_{42}}{4} & R_d &= \widetilde{R}_{34} = R_{24} + \frac{G_{34} - G_{14}}{2} \\ R_e &= \widetilde{R}_{35} = \frac{R_{24} + R_{26}}{2} + \frac{B_{35} - B_{15}}{2} & R_f &= R_{24} \\ R_g &= \widetilde{R}_{25} = \frac{R_{24} + R_{26}}{2} \end{aligned} \tag{1}$$

For B primary color pixels, the estimate of R color pixels in the context template are interpolated in the same manner as R primary color pixels.

(2) For G primary color pixels, the interpolation template is shown in Fig. 2(c). The estimate of G color pixels in the context template are given by:

$$\begin{aligned} R_a &= G_{32} & R_b &= \widetilde{G}_{33} = \frac{G_{32} + B_{33} - B_{31}}{2} + \frac{G_{23} + B_{33} - B_{13}}{2} \\ R_c &= G_{23} & R_d &= \widetilde{G}_{24} = \frac{\dfrac{G_{23} + G_{25}}{2} + G_{14} + \dfrac{R_{24} - R_{04}}{2}}{2} \\ R_e &= G_{25} & R_f &= G_{14} \\ R_g &= \widetilde{G}_{15} = \frac{G_{25} + G_{14} + G_{16} + G_{05}}{4} \end{aligned} \tag{2}$$

Taking advantage of spectral correlations of Bayer format image, Eqs (1) and (2) estimate the pixel values in the context template by only using previous pixels of the current pixel. So, the proposed method is called causal interpolation, which can be executed with simple additions and shifts, meeting the requirements of low-complexity.

To evaluate the influence of different interpolation methods to the distribution of prediction error, the peak signal-to-noise ratio is obtained with:

$$PSNR = 10 \lg \frac{255^2}{\dfrac{1}{3MN} \displaystyle\sum_{i=1}^{3} \sum_{x=1}^{M} \sum_{y=1}^{N} [I_1(x,y,i) - I_2(x,y,i)]^2} \tag{3}$$

Table 1
PSNR of proposed method and literature [18]

Image	Proposed method	Method in [18]
1	23.030	37.9855
2	28.196	42.2009
3	24.421	40.1568
4	26.782	38.4660
Average	25.607	39.702

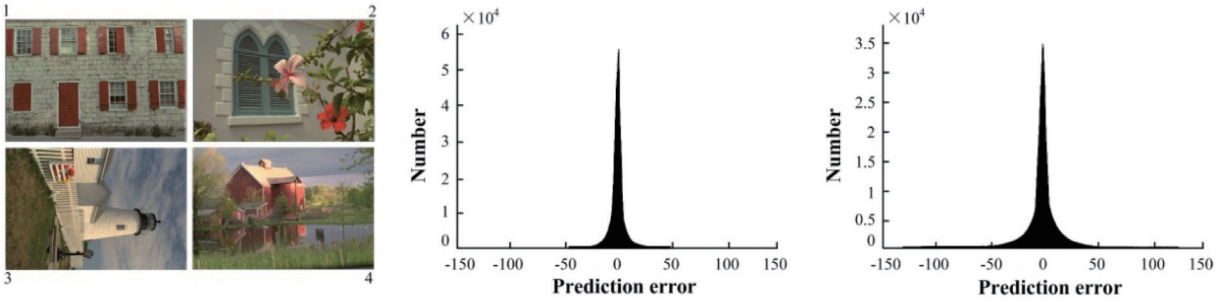

(a) (b) (c)

Fig. 3. The comparison of prediction error: (a) Kodak images, (b) prediction error of [18], (c) prediction error of causal interpolation.

where $i = 1, 2, 3$ denote the three primary color components; M, N are the height and width of the image. Compared to the interpolation method proposed in literature [18], the test results of PSNR after predicting correction of standard JPEG-LS with Kodak images in Fig. 3(a) are listed in Table 1.

From the table, it can be seen that the quality of the reconstructed images of causal interpolation is 14.1 dB lower than that of literature [18]. However, this does not indicate a significant difference in the distribution of prediction error. Figures 3(b) and (c) show the histogram distributions of prediction error in literature [18] and that obtained by the proposed method with image 3, respectively. The prediction errors are more concentrated near zero in the literature [18]. Although a better interpolation method leads to sharper distribution curves, which could potentially improve the coding efficiency, its complexity and non-causality determines that it cannot be applied in the design of one-pass encoder.

2.2. Gradient predictor

The distribution of the prediction error with causal interpolation expands on two sides away from zero, which is shown in Fig. 3(c). This means that the number of coding items increases, resulting in lower coding efficiency. A gradient predictor is designed to make up for this by improving the prediction accuracy. There are 7 pixels in the prediction template, shown in Fig. 2(a). The current pixel can be effectively predicted based on the gradient in the prediction template. If we analyzed the local gradient in the template, the gradient predictor presented here calculates the predictive value according to the gradient variation of the current pixel.

The steps of gradient prediction are as follows:

Step 1: Calculate the horizontal gradient:

$$Rh_1 = d - c$$

$$Rh_2 = b - a$$

$$Rh_3 = d - e \tag{4}$$
$$Rh = |Rh_1| + \frac{|Rh_2| + |Rh_3|}{2}$$

Step 2: Calculate the vertical gradient:

$$\begin{aligned} Rv_1 &= b - c \\ Rv_2 &= d - f \\ Rv_3 &= e - g \\ Rv &= |Rv_1| + \frac{|Rv_2| + |Rv_3|}{2} \end{aligned} \tag{5}$$

Step 3: Adaptively adjust the predictor according to the value of Rh and Rv:

$$\widehat{x}_{GRA} = \begin{cases} b + Rh_1, & Rv - Rh > T_3 \\ (b + Rh_2 + d + Rh_1)/2, & T_2 < Rv - Rh < T_3 \\ (b + d + Rh)/2, & T_1 < Rv - Rh < T_2 \\ b + d - c, & -T_1 < Rv - Rh < T_1 \\ (b + d + Rv)/2, & -T_2 < Rv - Rh < -T_1 \\ (b + Rv_1 + d + Rv_2)/2, & -T_3 < Rv - Rh < -T_2 \\ d + Rv_1, & Rv - Rh < -T_3 \end{cases} \tag{6}$$

where $\hat{x}_{GAR}$ is the predictive value; T_1, T_2, T_3 are gradient thresholds that are obtained through experiments.

During the process of prediction, comparisons, shifts, and additions are used. These methods can be easily implemented by hardware. The computational complexity is slightly higher than a median predictor, but the gradient predictor achieves a more accurate prediction in high-frequency regions of the image.

2.3. Gradient context optimization

The output of the gradient predictor should be further corrected based on a context model. In addition, the quantization performance of the context model directly determines the accuracy of the conditional probability estimate, thus affecting the coding efficiency. To acquire the optimal quantization interval, the context obtained from causal interpolation needs to be re-quantized for Bayer format images.

According to the theory of source coding, the least bit number of continuous encoding for sequence $x_1, x_2, \ldots, x_n$ is given by:

$$-\log_2 \prod_{i=1}^{n} p(x_i \mid x_{i-1}, \ldots, x_1), \quad 1 \leqslant i \leqslant n \tag{7}$$

Under the conditions of the context, the minimum entropy could be achieved. But in practice, the size and quantity of the context is limited, and a smaller size or quantity can reduce the cost of the model. The Lloyd iteration method [19] is adopted here with the minimum entropy as the cost function to re-quantize the context. The optimized context quantization intervals are determined as follows:

$$\{0\}, \pm\{1, 2, 3, 4\}, \pm\{5, 6, 7, 8, 9\}, \pm\{10, 11, \ldots, 25, 25, 27\}, \pm\{c \mid c \geqslant 28\} \tag{8}$$

The coding efficiency could be improved by 2%∼3% with these intervals.

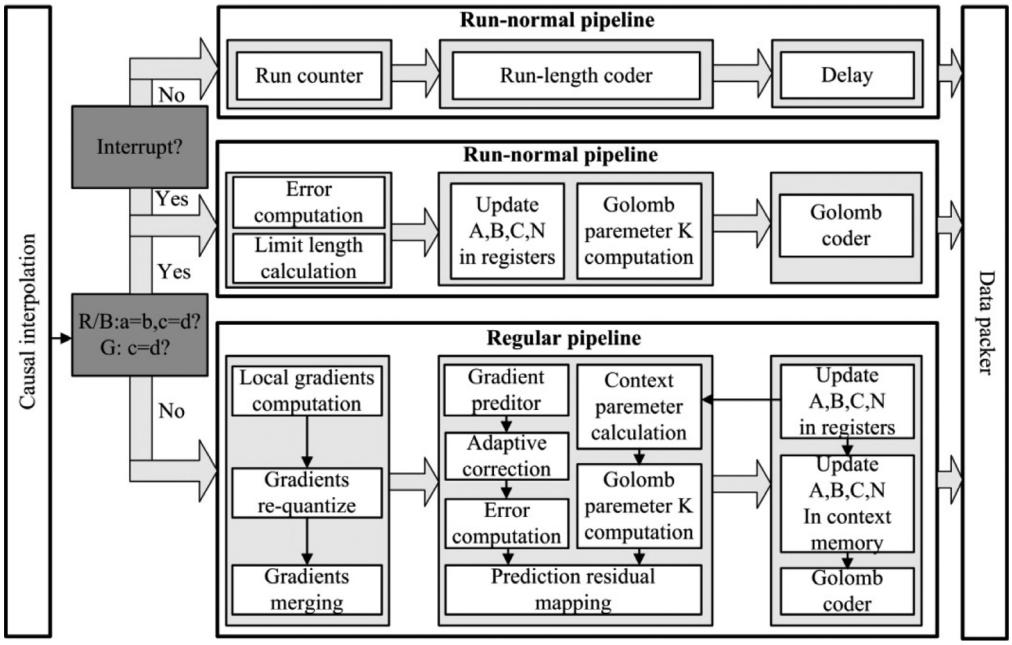

Fig. 4. Three parallel data paths inside the encoder.

2.4. Parallel data encoder

To minimize the resource utilization and power consumption, a complexity and power efficient data encoder should be designed for VLSI implementation. Three parallel data paths are adopted in our presented date encoder, as shown in Fig. 4. The three pipelines are the run-normal mode, the run-interruption state, and the regular mode. Only one pipeline is activated according to the mode determinations in the dark gray color, which avoid the unnecessary computation of the other two pipelines for each pixel.

Considering the similar background of WCE images, the processing time, the power consumption and the unnecessary switch of activities would be effectively reduced due to the low computation complexity in the pipeline. On the other hand, the common computation, such as the Golomb parameter k and the Golomb coder, could utilize the sharing of resources among pipelines, which might significantly reduce the gate counts.

3. Results

In our experiments, we compare the proposed near-lossless compression method with other methods developed from standard JPEG-LS compression to evaluate its performance. The tested Bayer format images are re-sampled from the five typical 24-bit color images with size 512×512. The comparison results are illustrated in Table 2.

Among the compression algorithms in Table 2, the proposed algorithm provides the highest average compression rate, as well as a high PSNR of 46.305 dB. The average compression rate is 2.315 in the five standard test images. We must note that the standard JPEG-LS lossless and near-lossless compression methods used with Bayer images have very low compression rates. The method presented in [5] is achieved according to the structure conversion of Bayer array to separate the three color components.

Table 2
Compression results for five test images

	Images (512 × 512)	Airplane	Baboon	House	Lenna	Pepper	Average
JPEG-LS lossless	PSNR (dB)	∞	∞	∞	∞	∞	∞
	CR	1.699	1.163	1.527	1.492	1.505	1.477
JPEG-LS near-lossless (near $= 2$)	PSNR (dB)	45.171	45.380	45.154	45.123	45.241	45.214
	CR	2.656	1.195	2.035	1.634	1.528	1.809
Method [5]	PSNR (dB)	46.411	46.389	46.427	46.407	46.546	46.428
	CR	2.682	1.629	2.303	2.309	2.268	2.238
Method [20]	PSNR (dB)	46.403	46.390	46.374	46.384	46.460	46.409
	CR	2.507	1.635	1.967	1.698	1.634	1.549
Proposed algorithm	PSNR (dB)	46.274	46.253	46.312	46.265	46.422	46.305
	CR	2.692	1.720	2.479	2.347	2.337	2.315

Note. CR means compression rate and ∞ means infinity.

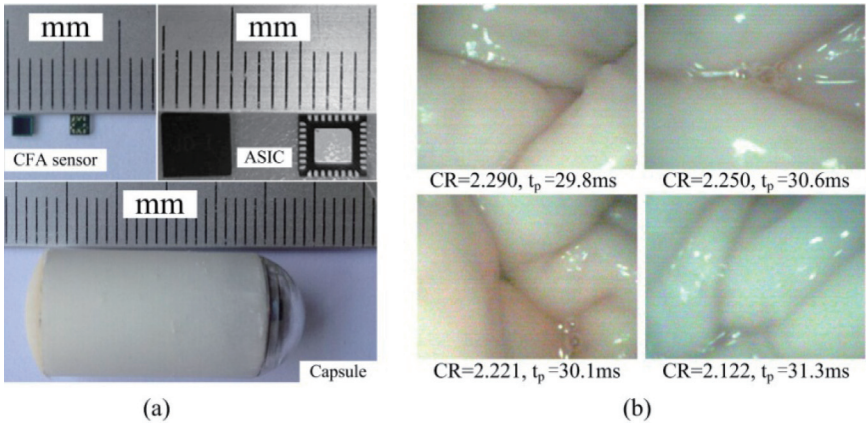

Fig. 5. The performance of proposed method in wireless capsule: (a) photos of modules inside the capsule, (b) compression rate (CR) and processing time (t_p) for actual pig's intestine images.

Then, the JPEG-LS near-lossless compression with *near* $= 2$ is used for R, G and B. The method provides a slightly lower compression rate, but a higher PSNR by 0.12 dB. However, the structure conversion method determines that it cannot satisfy one-pass mechanism, which means large storage resources. Compared to the compression method presented in [20], the new method improves the compression rate by 0.77 at the cost of a 0.1 dB decrease of PSNR. So, considering the trade-off between the compression rate and the image quality, the proposed compression method is more suitable for the wireless endoscopy system.

A wireless endoscopy system is designed based on the new compression algorithm proposed in this paper and is shown in Fig. 5(a). The CMOS sensor produced by OmniVision Technologies, Inc is adopted with a resolution of 400 × 400, and is in a digital parallel Bayer format output. The ASIC is fabricated in 0.18-μmCMOS technology with a die area of 5.0 mm × 5.0 mm. The whole size of the capsule is Φ 11 × 26 mm.

Under the High clock of 40 MHz, the performance of the proposed compression method in the designed capsule system is shown in Fig. 5(b). The full-color pig's intestine images are rendered by an edge-sensing demosaicing method [21]. The compression rate is acceptable, and the duration of the process is satisfactory.

4. Discussions and conclusion

As a key part of ASIC, the design of the compression method should comprehensively consider the computational complexity, the storage resources, the processing time, and the power consumption. In view of this, a complexity-efficient and one-pass image compression method suitable for an ASIC design based on Bayer format images has been presented. The average compression rate could reach 2.315 with a relatively high PSNR of 46.3 dB. The experimental and comparative results show that our new, near-lossless compression method performs better than any other method considering the numerous restrictions of wireless capsule endoscopy. It performs well in the designed wireless capsule system, reducing the bandwidth of image communication and allowing it to be applied to other fields.

The method proposed achieved considerable experimental and actual results. However, there are some drawbacks. Firstly, the PSNR in the proposed method displays little to no significant improvement when compared with other algorithms, which results from the rounding operation of shifts in causal interpolation and gradient prediction. Secondly, the actual compression rate is not as good as that in standard test images. The essence of JPEG-LS is predictive coding, so a higher resolution means a larger CR, as well as a more accurate diagnosis of GI diseases. Future studies will focus on optimizing the rounding operations and improving the resolution of the image sensor in the wireless capsule system.

Acknowledgements

This research was supported by the National Natural Science Foundation of China, No. 31170968, and Innovation Program of Shanghai Municipal Education Commission, No. 09DZ1907400.

References

[1] Iddan G, Meron G, Glukhovsky A et al. Wireless capsule endoscopy. Nature. 2000; 405(6785): 417-417.
[2] Pillcam. (2011). Given Imaging [Online]. Available: http://www.givenimaging.com/en-us.
[3] McCaffrey C, Chevalerias O, O'Mathuna C et al. Swallowable-capsule technology. Pervasive Computing, IEEE. 2008; 7(1): 23-29.
[4] Moglia A, Menciassi A, Dario P. Recent patents on wireless capsule endoscopy. Recent Patents on Biomedical Engineering. 2008; 1(1): 24-33.
[5] Chen X, Zhang X, Zhang L et al. A wireless capsule endoscope system with low-power controlling and processing ASIC. Biomedical Circuits and Systems, IEEE Transactions on. 2009; 3(1): 11-22.
[6] Wahid K, Ko S B, Teng D. Efficient hardware implementation of an image compressor for wireless capsule endoscopy applications. Neural Networks. 2008; 2761-2765.
[7] Khan T H, Wahid K A. Low power and low complexity compressor for video capsule endoscopy. Circuits and Systems for video technology, IEEE Transactions on. 2011; 21(10): 1534-1546.
[8] Ciuti G, Menciassi A, Dario P. Capsule endoscopy: from current achievements to open challenges. Biomedical Engineering, IEEE Reviews in. 2011; 4: 59-72.
[9] Koh C C, Mukherjee J, Mitra S K. New efficient methods of image compression in digital cameras with color filter array. Consumer Electronics, IEEE Transactions on. 2003; 49(4): 1448-1456.
[10] Li M M, Song Z J, Yang A P et al. Lossy compression of Bayer image with SPIHT. Industrial Electronics and Applications. 2011; 2244-2248.
[11] Chiu Y H, Chung K L, Yang W N et al. Universal intra coding for arbitrary RGB color filter arrays in HEVC. Journal of Visual Communication and Image Representation. 2013; 24(7): 867-884.
[12] Zhang N, Wu X. Lossless compression of color mosaic images. Image Processing, IEEE Transactions on. 2006; 15(6): 1379-1388.
[13] Poomrittigul S, Ogawa M, Iwahashi M et al. Reversible color transform for Bayer color filter array images. APSIPA Transactions on Signal and Information Processing. 2013; 2: e5.

[14] Xie X, Li G L, Wang Z H. A near-lossless image compression algorithm suitable for hardware design in wireless endoscopy system. EURASIP Journal on Applied Signal Processing. 2007; 2007(1): 48-48.
[15] Turcza P, Duplaga M. Low power FPGA-based image processing core for wireless capsule endoscopy. Sensors and Actuators A: Physical. 2011; 172(2): 552-560.
[16] Gu Y, Xie X, Li G et al. Two-stage wireless capsule image compression with low complexity and high quality. Electronics Letters. 2012; 48(25): 1588-1589.
[17] Chung K H, Chan Y H. A lossless compression scheme for Bayer color filter array images. Image Processing, IEEE Transactions on. 2008; 17(2): 134-144.
[18] Chang L, Tan Y P. Tan, Adaptive color filter array demosaicing with artifact suppression. Circuits and Systems, ISCAS'04. 2004; 3: 937-940.
[19] Lloyd S. Least squares quantization in PCM. Information Theory, IEEE Transactions on. 1982; 28(2): 129-137.
[20] Xie X, Li G, Wang Z. A low-complexity and high-quality image compression method for digital cameras. ETRI Journal. 2006; 28(2): 260-263.
[21] Hore A, Ziou D. An edge-sensing generic demosaicing algorithm with application to image resampling. Image Processing, IEEE Transactions on. 2011; 20(11): 3136-3150.